Available online at www.sciencedirect.com
SCIENCE DIRECT®
Journal of Sound and Vibration 291 (2006) 419–436
JOURNAL OF SOUND AND VIBRATION
www.elsevier.com/locate/jsvi

Vibration and guiding of moving media with edge weave imperfections

V. Kartik, J.A. Wickert*

Department of Mechanical Engineering, Carnegie Mellon University, Pittsburgh, PA 15213, USA

Received 15 December 2004; received in revised form 31 May 2005; accepted 16 June 2005
Available online 24 August 2005

Abstract

This paper examines the steady-state-forced vibration of a moving medium that is guided by a partial elastic foundation, and where geometric imperfections on the medium's edge act as an excitation source. Such a system is of technical interest in the areas of web handling and magnetic tape transport where externally pressurized air bearing guides are sometimes used to control lateral position. The axially moving strip is modeled here as a string that is guided by elastic foundation segments, and that is subjected to traveling wave excitation as the edge's imperfection interacts with the foundation. The equation of motion for this "moving medium and moving load" system incorporates a skew-symmetric Coriolis acceleration component that arises from convection. The governing equation is cast in state-space form, with one symmetric and one skew-symmetric operator, as is characteristic of gyroscopic systems. Through modal analysis, the forced response of the system is obtained to the complex harmonic excitation associated with the interaction between the edge's weave pattern and the guides. Parameter studies are presented in the transport speed, foundation stiffness, guide placement, guide width, and imperfection wavelength. Of potential technological application, for a given wavelength of the edge's imperfection, it is possible to reduce the medium's vibration at a certain location by judiciously selecting the locations and spans of the foundation segments.

*Corresponding author. Tel.: +1 412 268 2494; fax: +1 412 268 3348.
E-mail address: wickert@cmu.edu (J.A. Wickert).

0022-460X/$ - see front matter © 2005 Elsevier Ltd. All rights reserved.
doi:10.1016/j.jsv.2005.06.021

1. Introduction

The traveling string, beam, membrane, and plate are prototypical models for axially moving continua including magnetic tape libraries, automotive belt drives, power transmission chains, conveyor belts, and web transport systems in manufacturing. In some cases, the lateral motion of the medium is controlled through contact between its edge and one or more stationary guides. In the case of magnetic and optical tape libraries capable of storing petabytes of data, lateral motion of the tape arises from excitation sources such as the run-out of packs and rollers, or from impacts occurring between the tape and guiding flanges. Lateral motion is undesirable because it results in the misalignment of the data tracks and the read/write heads. High frequency lateral motion beyond the bandwidth of the track-following servo system is particularly problematic.

Externally pressurized air bearing guides, formed of a porous ceramic material, are one design option available for reducing such vibration. In Fig. 1, a slight taper θ to the bearing biases the lower edge of the tape against a flange that forms the guiding datum. A thin air film develops between the bearing's surface and the moving medium, and the lateral position is controlled by guiding against the datum surface. With this form of edge guiding, however, lateral motion can be influenced by imperfections or weave in the shape of the tape's edge. Deviation of the edge's shape from the straight ideal can excite vibration as the material convects over and interacts with the guide's flanges.

More generally, imperfections in the shape of a web or other moving medium can be introduced during the manufacturing process in which a wide web of material is slit into narrower portions. For instance, the aluminum sheet metal used in beverage containers is reduced in thickness in a rolling mill, coated, and then slit into narrower webs of a more suitable size for processing. Likewise, in the manufacture of magnetic tape, a web comprising a polymer substrate with magnetic and backside coatings is slit into narrower streams of tape, and these are subsequently wound onto data cartridges. In each case, the slitting process is accomplished by passing the

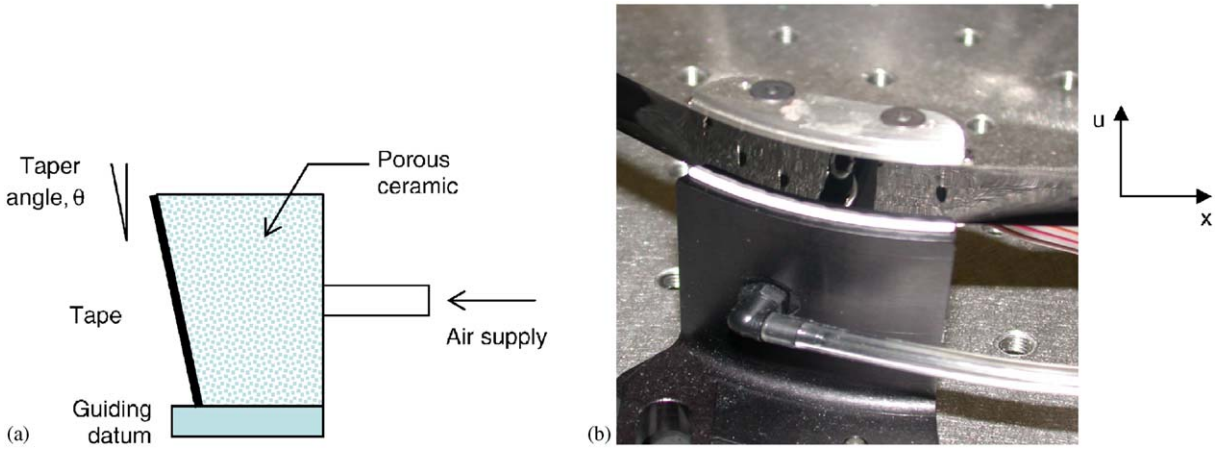

Fig. 1. (a) Cross-section of a guide having a pressurized air bearing surface formed of a porous ceramic material and a flange on the lower edge that establishes the reference datum for guiding. (b) Photograph of magnetic tape that is guided by such a bearing.

material through circular disk-like knives mounted on a rotating arbor, which in turn are received in coordinating grooves. In such a process, the vibration or non-flatness of those knives, or vibration of the web material itself, can be reproduced as a pattern of uneven edge shape. In some instances, periodic non-flatness of the knives maps directly to a sinusoidal weave pattern along the slit material's edge, and the wavelength of the imperfection is equivalent to the knife's circumference. When such materials are guided at high speed, the edge imperfection can act as a form of vibration excitation.

Previous work in the area of axially moving or translating continua has addressed the response to general forms of excitation by using modal analysis and Green's function methods [1–3]. In what follows, the interaction between the moving medium and the guiding datum is modeled as an elastic foundation. In that regard, application of the classical response methods for a traveling string on an elastic foundation is described in [4]. Other work in this area considers nonlinear free response [5] and the forced vibration of a traveling string on a foundation in the presence of boundary excitation [6]. Mode localization phenomena [7], the stability of moving media on elastic foundations at super-critical speeds [8,9], and the influence of a stationary load system [10] have also been examined. Certain studies have addressed the free and forced nonlinear vibration of viscoelastic moving belts [11,12] and traveling beams [13], the effect of excitation applied at support points [14,15], and in-plane vibration of a moving membrane [16]. Related work in the area of moving loads on moving media includes an investigation of the dynamics of translating strings with an attached mass [2,17] or with an attached damped oscillator [18].

The objective of this paper is to investigate the steady-state-forced response of moving media in the presence of edge guides and a sinusoidal imperfection. The medium is treated as a flexible strip that translates over (illustratively) two distributed guides that are modeled as elastic foundations. Vibration is excited through the moving load interaction of the strip's imperfection with the foundation. The dispersion afforded by the foundation's stiffness to the traveling strip becomes increasingly important as the transport speed increases. The equation of motion is cast in state-space form having one symmetric and one skew-symmetric operator, and the solution of the complex eigenvalue problem yields the system's mode shapes and natural frequencies. The modal analysis procedure for gyroscopic systems is applied to obtain the strip's response to the moving load-type excitation that arises as the medium convects over its guides. Parameter studies capture the influence of translation speed, foundation stiffness, and geometry on the strip's free and forced vibration.

2. Vibration with edge imperfection excitation

The axially moving strip shown in Fig. 2 is modeled as a flexible string that travels with tension T between the fixed supports located at $x = \pm(a + b + c)$, at which point the string's displacement vanishes. The strip's position is further controlled by distributed guides in the regions $x = (-(b + c), -c)$ and $x = (c, b + c)$ which are modeled as elastic foundations having stiffness k per unit length. In what follows, the guided and unguided spans of the strip are sequentially denoted $j = 1, 2, \ldots, 5$ beginning with the free span $j = 1$ in $x = (-(a + b + c), -(b + c))$.

The strip has nominal width h and thickness d, and it is pre-loaded against the foundation by the downward force p per unit length. In a guide having the design of Fig. 1, the preload is

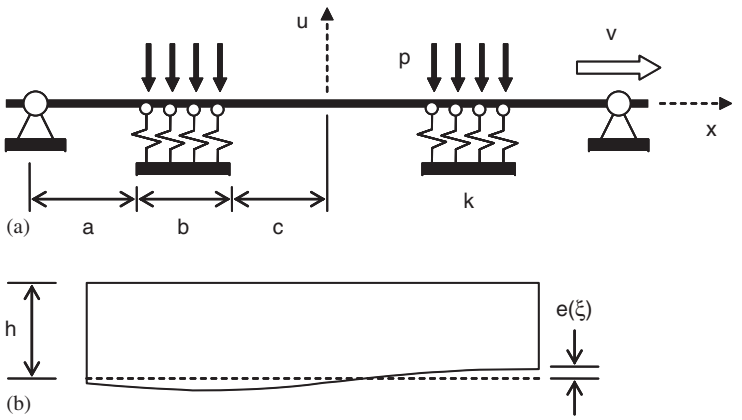

Fig. 2. (a) Schematic of the vibration model for a moving strip having its lateral motion controlled by two distributed guides. (b) Detail of imperfection on the strip's edge.

developed by tilting the bearing's surface by the slight angle θ. With the strip encircling the guide over the wrap angle ϕ, the preload

$$p = \frac{T}{r}\,\phi\,\sin\,\theta \tag{1}$$

biases the strip against the guide's lower flange, where the guide's radius of curvature is denoted by r.

When the strip's edge is not straight, deviation of the width from its nominal value is represented by $e(\xi)$, where the coordinate ξ is measured in a reference frame that is fixed in the strip. The edge's defect has amplitude ε and wavelength L, and it is taken as

$$e(\xi) = \varepsilon\,\cos\left(\frac{2\pi}{L}\,\xi\right). \tag{2}$$

This form is representative of the weave distortion in a web's edge that is produced by slitting manufacturing operations using rotating circular knives. The geometrical defect (2) travels with the strip, and it can excite vibration as the edge moves across, and interacts with, the guides of stiffness k. The amplitude of steady-state vibration that is present in the unguided span $x = (-c, c)$ depends on the length b of the guides, the wavelength L of the imperfection, and the other model parameters that are listed in Table 1.

The strip travels at the constant speed v relative to the ground-based coordinate x, and in Eq. (2), $\xi = x - vt$. With deflection u in the direction orthogonal to the tape's translation, the equation of motion is

$$\rho A\left(u_{,tt} + 2vu_{,xt} + v^2u_{,xx}\right) - Tu_{,xx} + kH(x)(u + e) = -pH(x), \tag{3}$$

where ρ is the strip's mass density, and $A = hd$ is its cross-sectional area. Here $H(x)$ is a windowing function that is set to unity over the guides and is zero otherwise. The width change is specified to be sufficiently small that variations in the strip's mass per unit length, and in particular, their influence on potential parametric resonances are negligible. In a Eulerian

Table 1
Nominal values of parameters used in the case studies

Density, ρ	1400 kg/m^3
Tension, T	1 N
Speed, v	10 m/s
Foundation stiffness, k	5000 N/m^2
Width, h	12.7 mm
Thickness, d	6.5 μm
Lengths	
a	63.60 mm
b	38.10 mm
c	19.05 mm
Imperfection amplitude, A	1 μm
Guide taper angle, θ	0.6°
Imperfection wavelength, L	250 mm

formulation with the ground-based reference frame x, an element of the strip experiences local, Coriolis, and centripetal acceleration components. By defining the mass M, gyroscopic G, and stiffness K operators

$$M = \rho A \bullet, \tag{4}$$

$$G = 2v\rho A \frac{\partial}{\partial x} \bullet, \tag{5}$$

$$K = -(T - \rho A v^2)\frac{\partial^2}{\partial x^2} \bullet + kH(x) \bullet, \tag{6}$$

the equation of motion is written in the symbolic form

$$Mu_{,tt} + Gu_{,t} + Ku = f \tag{7}$$

for gyroscopic dynamic systems. Bending of the strip can be incorporated in the strip's model through appropriate modification of K. With respect to the inner product

$$\langle g_1, g_2 \rangle = \int_{-(a+b+c)}^{a+b+c} g_1 g_2 \, \mathrm{d}x \tag{8}$$

for two functions g_1 and g_2 having zero displacement at the supports, operators M and K are self-adjoint and positive definite for transport speeds below $v_c = \sqrt{T/(\rho A)}$. The operator G is skew-symmetric. The dynamics of gyroscopic systems are further discussed in references [19,20].

The supports and the datum $u = 0$ are henceforth set to the position at which the guides are uniformly compressed by amount p/k. The excitation in Eq. (7) then becomes

$$f = -ke(x - vt)H(x) = -k\varepsilon \sin\left(\frac{2\pi}{L}(x - vt)\right)H(x), \tag{9}$$

which convects with the strip, has wavenumber $2\pi/L$, and circular frequency $2\pi v/L$.

3. Natural frequencies and modes

The forced response of the strip to the moving load edge excitation is determined through modal analysis for gyroscopic systems. In the spans $(-(a+b+c),-(b+c)),(-c,c)$, and $(b+c,a+b+c)$, the free vibration solutions have the form

$$u(x,t)=\mathrm{e}^{\lambda t+\gamma x}, \tag{10}$$

where $\lambda=\mathrm{i}\omega$, $\mathrm{i}^2=-1$, and ω is the circular natural frequency. The dispersion relation in those spans is

$$-(v_c^2-v^2)\gamma^2+(2v\lambda)\gamma+\lambda^2=0, \tag{11}$$

where the wavenumbers γ are

$$\gamma_1=-\frac{\lambda}{v_c+v} \quad \text{and} \quad \gamma_2=\frac{\lambda}{v_c-v}. \tag{12}$$

An eigenfunction in an unguided span ($j=1,3$, and 5) becomes

$$\psi_{\text{free}}=C_1^{(j)}\exp\left(\frac{-\lambda}{v_c+v}x\right)+C_2^{(j)}\exp\left(\frac{\lambda}{v_c-v}x\right), \tag{13}$$

where $C_1^{(j)}$ and $C_2^{(j)}$ are constants. In the guided spans $(-(b+c),-c)$ and $(c,b+c)$, the dispersion relation

$$-(v_c^2-v^2)\gamma^2+(2v\lambda)\gamma+(\lambda^2+k^2)=0 \tag{14}$$

includes a contribution from the elastic foundation and has roots

$$\gamma_1=\alpha+\beta \quad \text{and} \quad \gamma_2=\alpha-\beta, \tag{15}$$

where

$$\alpha=\frac{v\lambda}{v_c^2-v^2}, \tag{16}$$

$$\beta=\frac{1}{v_c^2-v^2}\sqrt{v_c^2\lambda^2+\left(v_c^2-v^2\right)\frac{k}{\rho A}}. \tag{17}$$

The eigenfunction in a guided span ($j=2$ and 4) then takes the form

$$\psi_{\text{guided}}=\mathrm{e}^{\alpha x}\left(C_1^{(j)}\mathrm{e}^{-\beta x}+C_2^{(j)}\mathrm{e}^{\beta x}\right). \tag{18}$$

In the light of Eq. (17), the character of the eigenfunction in a guided span depends on the guide's stiffness. While α is always imaginary, the cut-off frequency

$$\omega_c=\sqrt{\left(1-\left(\frac{v}{v_c}\right)^2\right)\left(\frac{k}{\rho A}\right)} \tag{19}$$

demarcates frequency ranges over which β is real ($\omega<\omega_c$), zero ($\omega=\omega_c$), and imaginary ($\omega>\omega_c$). Precisely at the cut-off frequency, $\gamma_1=\gamma_2$, and the prospective eigenfunction

takes the form

$$\psi_{\text{cut-off}} = \left(C_1^{(j)} + C_2^{(j)} x\right) \mathrm{e}^{\alpha x} \tag{20}$$

with exponent

$$\alpha = \frac{\mathrm{i} v \omega_c}{v_c^2 - v^2}. \tag{21}$$

In Eqs. (13), (18) and (20), the constants $C_1^{(j)}$ and $C_2^{(j)}$ can be complex, and they are determined through the boundary conditions, displacement, and slope compatibility relations among neighboring spans. Those requirements yield a set of ten homogeneous, linear, algebraic equations that define the system-level characteristic equation. Natural frequencies and the coefficients $C_i^{(j)}$ in the mode shapes are obtained numerically.

The influence of the guide's stiffness on the natural frequency spectrum is depicted in Fig. 3. In this parameter study, stiffness is varied with all other parameters being held constant at the nominal values in Table 1. As the stiffness is increased, each natural frequency increases, and certain pairs of frequencies coalesce at high stiffness values. At $k = 0$, the natural frequencies reduce to the classical values expected for an axially moving string [1]. Each natural frequency at $k = 0$ exceeds ω_c, but as the foundation's stiffness increases, the cut-off frequency grows at a faster rate than the lower natural frequencies. Depending on the mode and transport speed, the eigenfunction can therefore assume different functional forms in the light of Eq. (17). For the configuration of Fig. 2 in which two guides are present and three spans couple, the loci for modes $3(i-1)+1$ and $3(i-1)+2$, where $i = 1, 2, 3 \ldots$, coalesce at higher values of the foundation's stiffness. Likewise, the locus for mode $3(i-1)+3$ remains distinct from the others.

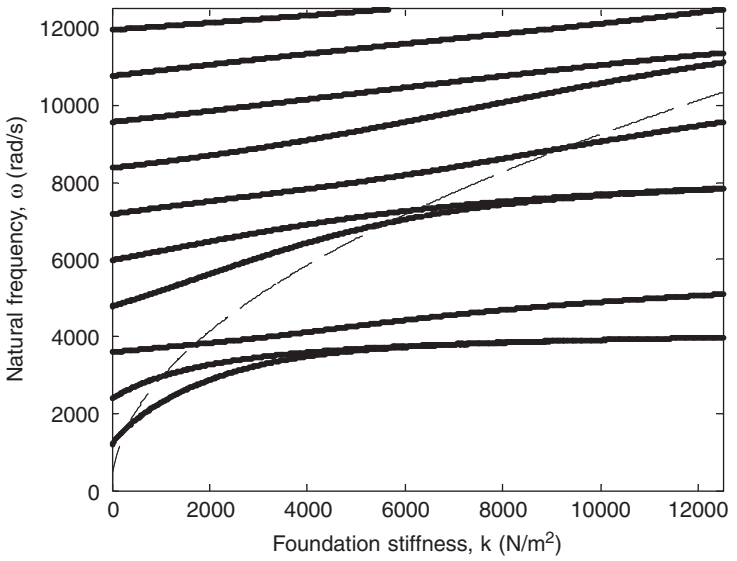

Fig. 3. Loci of natural frequencies (bold line type), and the cut-off frequency (dashed line type), as functions of the guides' stiffness. The other parameters are held constant at the values listed in Table 1.

The cut-off frequency is always a root of the characteristic equation, which is formed as the determinant of the matrix involving the $C_i^{(j)}$. However, based on the functional form (20) that is taken by the eigenfunction at ω_c, non-trivial solutions for the eigenfunction that satisfy the boundary and compatibility conditions do not exist, and so ω_c is not a natural frequency at any value of k. The cut-off frequency simply demarcates frequency ranges where the spatial character of the mode shape changes functional form.

The first four mode shapes of the strip are shown in Fig. 4 at the illustrative value $k = 5000\,\mathrm{N/m^2}$ (the normalization scheme for the eigenfunctions is described below in Eq. (33)). Because of the strip's convection, the eigenfunctions are complex, and they introduce a spatial phase shift to the strip's vibration. The shapes are further distorted relative to those of an un-guided traveling strip owing to the constraints that are imposed by the guides. The elastic foundation segments reduce the modal displacement in the guided regions, and shift regions of higher amplitude to the un-guided spans. Fig. 5 depicts the manner in which the magnitudes $|\psi|$ of the first three complex mode shapes vary with the foundation's stiffness. At $k = 0$, the mode shapes are proportional to

$$\psi = \sin\left(\frac{n\pi x}{2(a+b+c)}\right)\exp\left(\mathrm{i}\frac{n\pi v x}{2v_c(a+b+c)}\right), \tag{22}$$

where $n = 1, 2, \ldots$. Likewise, the natural frequencies are integer multiples and well-separated from one another as indicated in Fig. 3. When the stiffness is increased to $k = 2000\,\mathrm{N/m^2}$, the frequencies remain distinct but are separated from one another by only 14%. In turn, the strip's

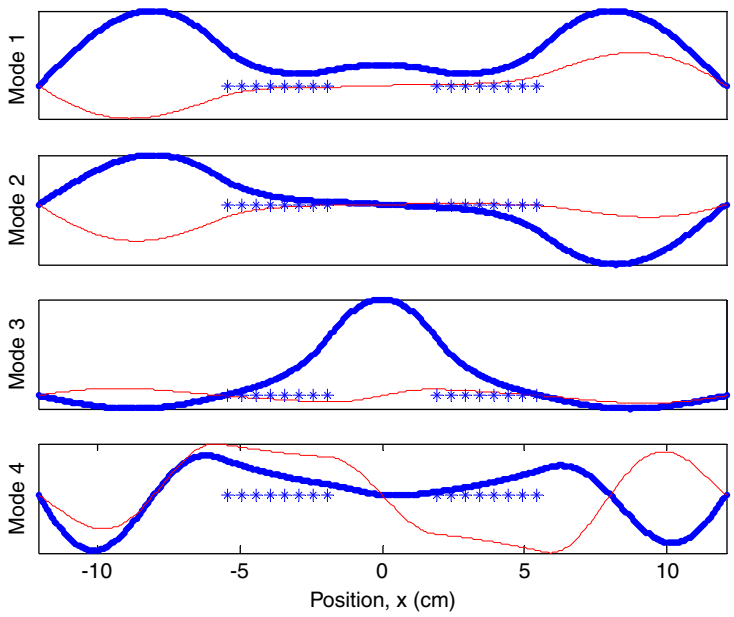

Fig. 4. First four mode shapes of the guided strip; $k = 5000\,\mathrm{N/m^2}$. Real components are shown in bold line type, and imaginary components in light line type. The locations of the guides are indicated by the hatched regions.

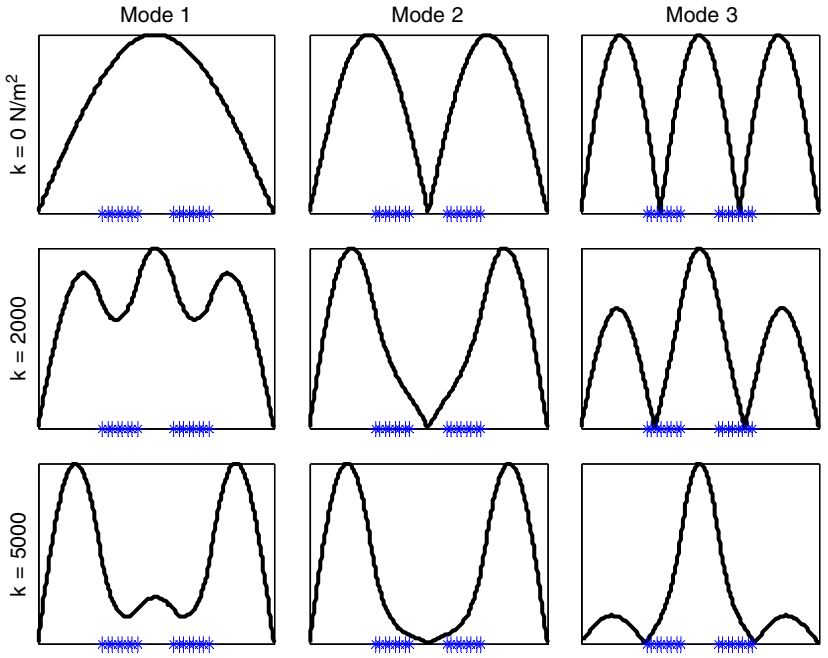

Fig. 5. Magnitudes of the strip's first three mode shapes for different values of the foundation stiffness; $k = 0$, 2000 and 5000 $\mathrm{N/m^2}$. The locations of the guides are indicated by the hatched regions.

displacement is reduced in the first and second modes over the guided regions as indicated in the second row of Fig. 5. At the higher foundation stiffness of $k = 5000\,\mathrm{N/m^2}$, the first and second natural frequencies are separated by only 2%. In the third row of Fig. 5, the first and second modes become qualitatively similar in appearance. Each has reduced displacements over the guides and the central un-guided span, and these modes are differentiated primarily by phase differences in the un-guided spans. For sufficiently high stiffness, the first two modes coalesce in frequency and are characterized by large motions in the outlying spans, with little or no motion occurring over the guides and the central free span. The third mode, of distinct frequency, is characterized by large amplitude motion in the central span. A similar structure exists for the next three vibration modes, with the fourth and the fifth frequencies coalescing while the sixth remains distinct. The qualitative character of higher modes repeats in such groups of three.

Fig. 6 depicts the effect of the strip's transport speed on its natural frequencies, and on the cut-off frequency. The excitation frequencies corresponding to different wavelengths of edge defect are also shown in the figure as load lines, as described in the following section. The natural frequencies of the strip-guide system and ω_c decrease monotonically with v. The first two natural frequencies differ by less than 3% when the tape is stationary, and coalesce further as the tape transport speed increases. The first three natural frequencies are below the cut-off frequency over much of the speed range shown in Fig. 6, and they differ in functional form from the higher modes following Eqs. (16)–(18).

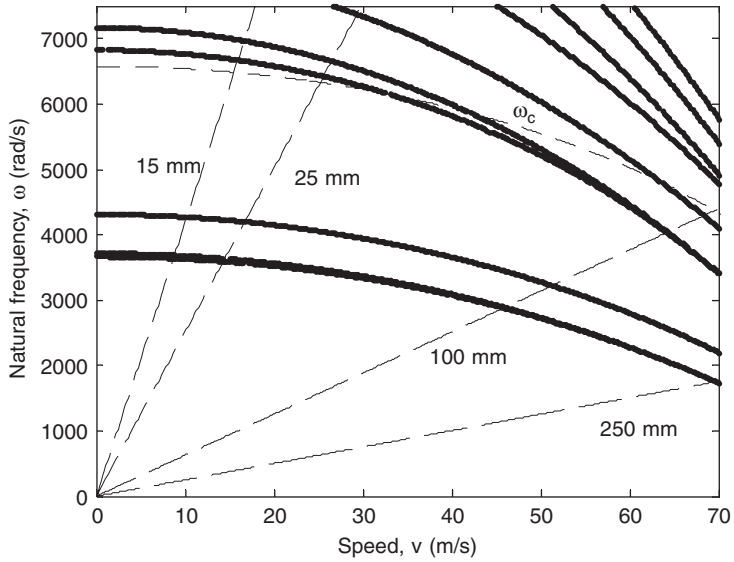

Fig. 6. Loci of natural frequencies (bold line type), and the cutoff frequency (dashed line type), as functions of speed. The excitation frequencies corresponding to edge defects of wavelengths of 15, 25, 100, and 250 mm are also shown (dotted line type). The other parameters are held constant at the values listed in Table 1.

4. Response to traveling wave loading

The forced response to moving load excitation associated with a harmonic edge defect is considered next. The eigenfunctions ψ are not orthogonal with respect to M, G, and K individually, but the equation of motion can be re-cast in an alternative format that is amenable to modal analysis. With the definition of the state and excitation vectors

$$\underline{w} = \begin{Bmatrix} u_{,t} \\ u \end{Bmatrix}, \tag{23}$$

$$\underline{q} = \begin{Bmatrix} f \\ 0 \end{Bmatrix} \tag{24}$$

the equation of motion is written in the first-order form

$$\underline{A}\,\underline{w}_{,t} + \underline{B}\,\underline{w} = \underline{q} \tag{25}$$

with the matrix differential operators

$$\underline{A} = \begin{bmatrix} M & O \\ O & K \end{bmatrix}, \tag{26}$$

$$\underline{B} = \begin{bmatrix} G & K \\ -K & 0 \end{bmatrix}. \tag{27}$$

Here the underscore denotes either a vector or matrix quantity. Operator A is symmetric, and B is skew-symmetric, with respect to the inner product

$$\left(\underline{g}_1, \underline{g}_2\right) = \int_{-(a+b+c)}^{a+b+c} \underline{g}_2^{\mathrm{T}} \underline{g}_1 \, \mathrm{d}x, \tag{28}$$

which is defined in terms of vector test functions g_1 and g_2 that satisfy zero displacement conditions at the supports. Free vibration solutions

$$\underline{w}(x,t) = \mathrm{e}^{\lambda t} \, \underline{\phi}(x) \tag{29}$$

satisfy the eigenvalue problem

$$\lambda \, \underline{A} \, \underline{\phi} + \underline{B} \, \underline{\phi} = 0 \tag{30}$$

for the eigenvalue λ and vector eigenfunction ϕ. In terms of the scalar ψ, the state representation of each mode is

$$\underline{\phi} = \left\{ \begin{array}{c} \lambda\psi \\ \psi \end{array} \right\}. \tag{31}$$

With $\lambda_n = \mathrm{i}\omega_n$ for $n \geqslant 1$, the ω_n are real, positive, and ordered in an increasing sequence. To represent the modal response in a compact manner, the series is extended to negative indices with the definitions

$$\lambda_{-n} = \bar{\lambda}_n \quad \text{and} \quad \underline{\phi}_{-n} = \bar{\underline{\phi}}_n \tag{32}$$

for $n = 1, 2, \ldots$, where the overbar denotes complex conjugation. The state eigenfunctions are normalized with respect to A, and they are orthogonal with respect to operators A and B following

$$\left(\underline{A} \, \underline{\phi}_n, \underline{\phi}_m\right) = \delta_{nm}, \tag{33}$$

$$\left(\underline{B} \, \underline{\phi}_n, \underline{\phi}_m\right) = -\lambda_n \delta_{nm} \tag{34}$$

for $n, m = \pm 1, \pm 2, \pm 3, \ldots$.

The response of the strip is expressed as the expansion

$$\underline{w}(x,t) = \sum_{n=\pm 1, \, \pm 2 \ldots} \eta_n(t) \underline{\phi}_n(x) \tag{35}$$

and the generalized coordinate for each mode responds according to

$$\eta_n(t) = \eta_n(0) \mathrm{e}^{\lambda_n t} + \int_0^t \mathrm{e}^{\lambda_n (t-\tau)} N_n(\tau) \, \mathrm{d}\tau. \tag{36}$$

Here the initial values of the modal coordinates are given by

$$\eta_n(0) = (\underline{A} \, \underline{w}_0, \underline{\phi}_n), \tag{37}$$

where $w_0 = w(x,0)$, and the modal forces are

$$N_n(t) = (\underline{q}, \underline{\phi}_n). \tag{38}$$

In the present case, the excitation associated with interaction between the strip's edge and the guides is given in complex form by

$$f(x,t) = f_0(x)\mathrm{e}^{\mathrm{i}\omega t} + \text{c.c.}, \tag{39}$$

where the excitation frequency is

$$\omega = \frac{2\pi v}{L} \tag{40}$$

and the notation "c.c." denotes complex conjugates of the preceding terms. Following Eq. (9), the excitation's spatial distribution is

$$f_0 = -\frac{1}{2}\, k\varepsilon \exp\left(-\mathrm{i}\,\frac{2\pi}{L}\, x\right) H(x). \tag{41}$$

The steady-state forced response of the strip to the moving edge load then becomes

$$u(x,t) = \mathrm{e}^{\mathrm{i}\omega t}\left(\sum_{n=1,2,\ldots} \frac{(f_0, \psi_n)}{1-\omega/\omega_n}\, \psi_n(x) + \frac{(f_0, \bar{\psi}_n)}{1-\omega/\omega_n}\, \overline{\psi}_n(x)\right) + \text{c.c.} \tag{42}$$

for $\omega \neq \omega_n$.

From the standpoint of the steady-state forced response amplitude, the relative lengths of the strip's guided and un-guided spans, and their relation to the wavelength of the edge imperfection,

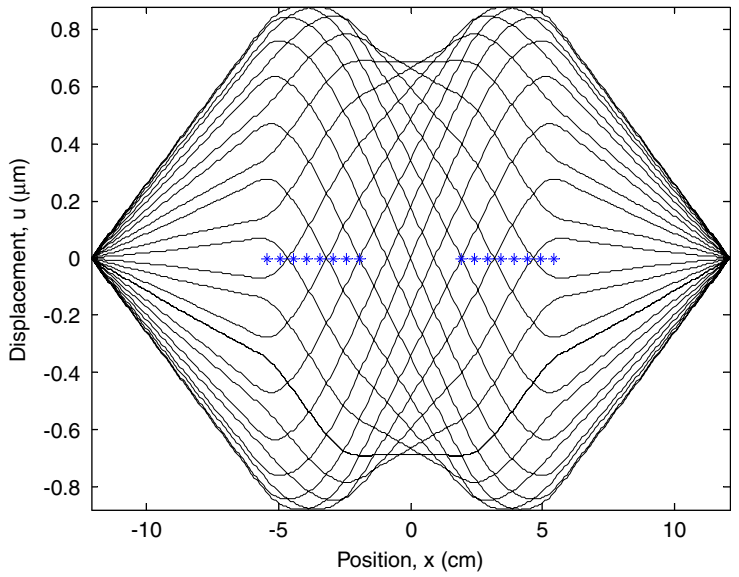

Fig. 7. Deflection of the strip at various time instants over one cycle of excitation; $L = 250$ mm. The locations of the guides are indicated by the hatched regions.

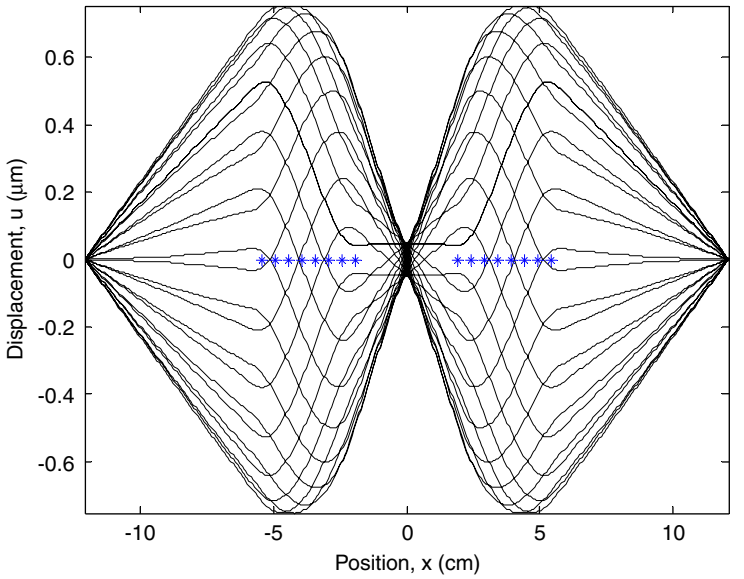

Fig. 8. Deflection of the strip at various time instants over one cycle of excitation; $L = 120\,\text{mm}$. The locations of the guides are indicated by the hatched regions.

are of particular interest. The strip's deflections at a number of time instants spaced over one cycle of excitation are shown in Figs. 7, 8, 10 and 11 for various wavelengths of the edge's imperfection.

In Fig. 7, where $L = 250\,\text{mm}$ and the amplitude of the defect is $1\,\mu\text{m}$, the strip's peak amplitude at mid-span is $0.66\,\mu\text{m}$. For the longer-wavelength defects, the strip responds nearly statically, and its peak amplitude is similar to the magnitude of the edge defect itself. In Fig. 8, the defect's wavelength has been reduced to $L = 120\,\text{mm}$. In this case, the maximal response along the strip is similar to that in Fig. 7, although the magnitude at mid-span is substantially reduced. The response is driven predominantly by the second vibration mode, for which the mid-point of the strip is a node, and the peak amplitude at mid-span is considerably lower than the magnitude of the imposed edge defect.

Fig. 9 depicts the manner in which the strip's response amplitude at mid-span changes over a wide range of imperfection wavenumbers $2\pi/L$. Here the dimensions of the spans and other parameters are held constant at the nominal values of Table 1. Certain wavenumbers exist at which the amplitude of the strip's vibration at the mid-span point vanishes, while for other wavenumbers, the response amplitude is maximized. Near wavenumbers 360 and $420\,\text{m}^{-1}$ for the parameters considered here, the strip resonates and the response is singular.

In Fig. 10 for wavelength $L = 33\,\text{mm}$, the response is driven by the fourth mode, and the strip's deflection at mid-span is reduced to less than 0.4% of the excitation's amplitude. For $L = 15\,\text{mm}$ in Fig. 11, resonance is excited and the peak amplitude at the mid-span is much greater than the amplitude of the edge defect. The response is dominated by the third mode, with the nodal points lying at the edge of each guide that is closer to the fixed supports, and the mid-point of the strip being an anti-node. The operating points corresponding to the responses shown in Figs. 7, 8, 10 and 11 are highlighted in Fig. 9.

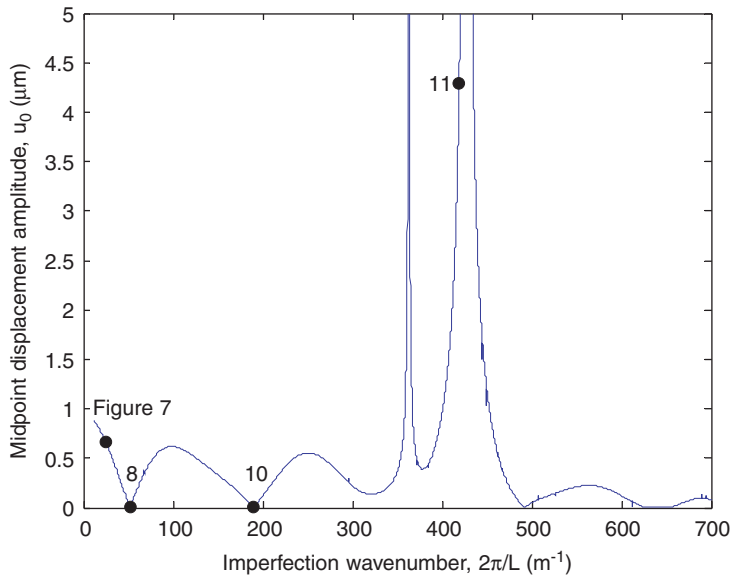

Fig. 9. Amplitude of steady-state vibration at the strip's mid-span point as a function of the edge imperfection's wavenumber; $x = 0$. The other parameters are held constant at the values listed in Table 1. The data points marked on the curve correspond to the motions depicted in Figs. 7, 8, 10 and 11.

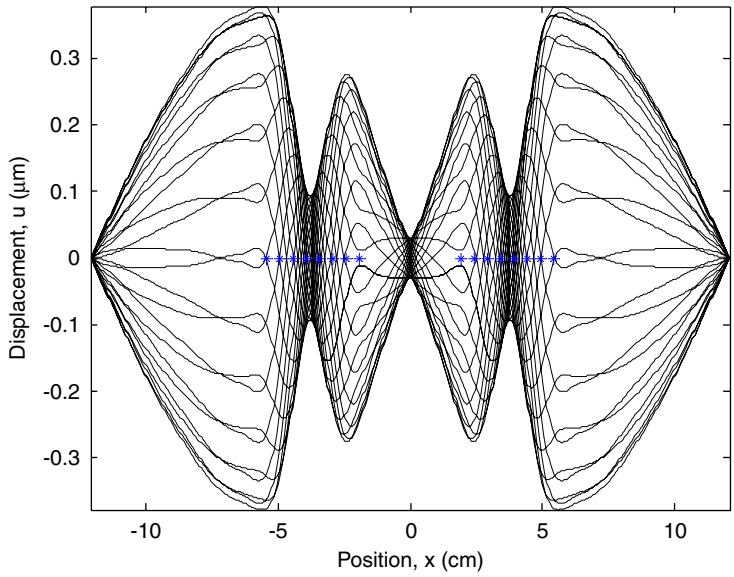

Fig. 10. Deflection of the strip at various time instants over one cycle of excitation; $L = 33$ mm. The locations of the guides are indicated by the hatched regions.

In some applications, it is desirable for a designer to select the geometry of the guides in order to reduce vibration occurring at a particular location of interest, to the extent that the wavelength of the edge defect is known from the specifics of the manufacturing process. When the edge

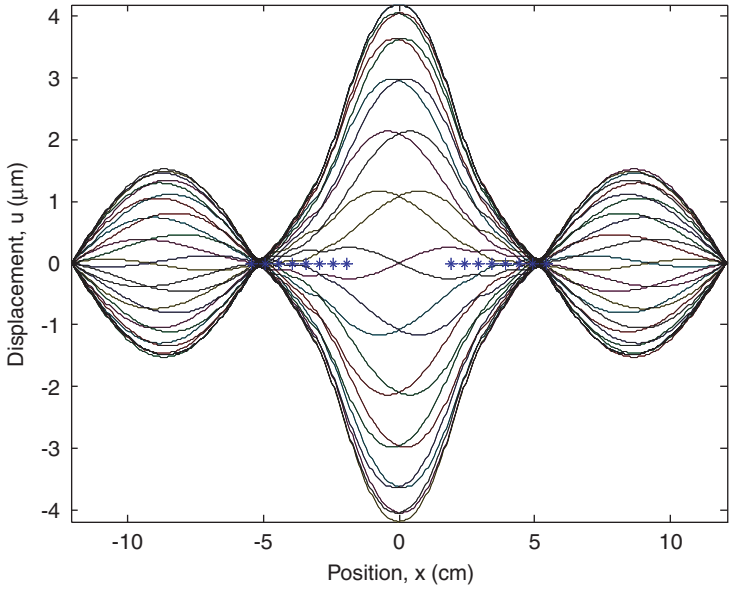

Fig. 11. Deflection of the strip at various time instants over one cycle of excitation; $L = 15$ mm. The locations of the guides are indicated by the hatched regions.

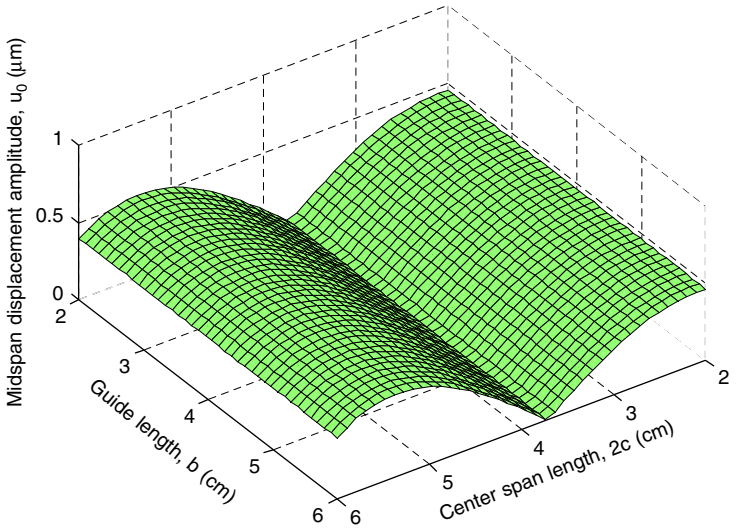

Fig. 12. Amplitude of steady-state vibration of the strip's mid-span point as a function of the central span's length $2c$ and the guide's length b; $x = 0$ and $L = 33$ mm. The other parameters are held constant at the values listed in Table 1.

imperfection arises from the slitting process during a manufacturing operation, the wavelength is often associated with the circumference of the slitting knives. In such an application, the design objective would be to minimize the vibration amplitude at locations where important processing

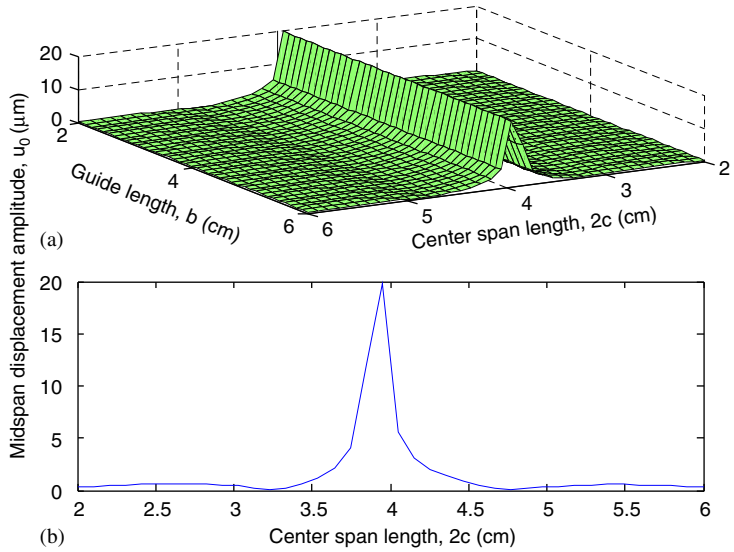

Fig. 13. (a) Amplitude of steady-state vibration at the strip's mid-span point as a function of the center span's length $2c$ and the guide's length b; $x = 0$ and $L = 15$ mm. The other parameters are held constant at the values listed in Table 1. (b) Section taken at the nominal value of the guide's length.

steps occur. In the case of a magnetic tape library, for instance, the width b of the guides, and the dimensions a and c of the free spans, can be chosen to reduce vibration amplitude at the location of the read/write heads. Thus, the designer could have leeway in selecting the transport path's geometry, even while such other parameters as speed, tension, and media wavelength are constrained by other considerations.

Figs. 12 and 13 depict the effect of varying dimensions b and c on the forced response amplitude at mid-span, illustratively for wavelengths $L = 33$ and 15 mm. In these parameter studies, the total length of the strip is held constant at the nominal value of Table 1. For longer wavelengths, the response amplitude is largely insensitive to the foundation's length b, but it decreases monotonically as the center span's length $2c$ is increased. In that instance, the imperfection's wavelength is larger than the strip's total length, and less than one wavelength of the disturbance can extend across the center span's length. The response amplitudes for imperfection wavelengths 33 mm (Fig. 12) and 15 mm (Fig. 13), however, do exhibit distinct local minima and peaks as b and c are varied. The displacement amplitudes are insensitive to the length of the elastic foundations to the extent that the effect of the foundation guides is to restrict the amplitude of motion over the guided span. The excitation wavelength of 15 mm excites a resonance of the system that accounts for the magnification of the response at a center span length of close to 3.9 cm. A section of Fig. 13(a) taken at the nominal value of the guide length b (Fig. 13(b)) indicates that zeros exist in the response for center span lengths near 3.2 and 4.7 cm, which are nearly integer multiples of the excitation's wavelength. In short, dimensional changes to a transport system's geometry can be optimized to reduce vibration of moving media that are positioned by edge guides.

5. Summary

This paper emphasizes the steady-state forced vibration of moving media in the presence of geometric edge imperfections that act as a source of excitation when the medium moves over a guide. This excitation takes the functional form of traveling wave loading to the extent that it convects with the medium. The response is found formally by employing a modal analysis procedure for gyroscopic dynamic systems. The nature of the response is influenced by a cut-off frequency which is shown to be distinct from the natural frequencies of the strip-foundation system. Parameter studies are performed with system variables such as foundation stiffness, transport speed, and strip and guide geometries to identify those design variables that significantly influence the response, and that can be optimally adjusted to minimize vibration at certain critical locations.

Acknowledgments

This work was supported by Imation Corporation through the MultiTerabyte Tape Storage program. The authors appreciate the assistance of Ted Schwarz, Richard Jewett, Chris Goldsmith, Steve Gavit, and Peter Groel with the work described herein.

References

[1] J.A. Wickert, C.D. Mote Jr., Classical vibration analysis of axially moving continua, *ASME Journal of Applied Mechanics* 57 (3) (1990) 738–744.
[2] J.A. Wickert, C.D. Mote Jr., Traveling load response of an axially moving string, *Journal of Sound and Vibration* 149 (2) (1991) 267–284.
[3] J.A. Wickert, C.D. Mote Jr., Response and discretization methods for axially moving materials, *ASME Applied Mechanics Reviews* 44 (11) (1991) 279–284.
[4] J.A. Wickert, Response solutions for the vibration of a traveling string on an elastic foundation, *ASME Journal of Vibration and Acoustics* 119 (1994) 137–139.
[5] R.B. Bhat, G.D. Xistris, T.S. Sankar, Dynamic behavior of a moving belt supported on elastic foundation, *ASME Journal of Mechanical Design* 104 (1982) 143–147.
[6] N.C. Perkins, Linear dynamics of a translating string on an elastic foundation, *ASME Journal of Vibration and Acoustics* 112 (1990) 2–7.
[7] C.A. Tan, L. Zhang, Dynamic characteristics of a constrained string translating across an elastic foundation, *ASME Journal of Vibration and Acoustics* 116 (1994) 318–325.
[8] R.K. Jha, R.G. Parker, Spatial discretization of axially moving media vibration problems, *ASME Journal of Vibration and Acoustics* 122 (2000) 290–294.
[9] R.G. Parker, Supercritical speed stability of the trivial equilibrium of an axially moving string on an elastic foundation, *Journal of Sound and Vibration* 221 (2) (1999) 205–219.
[10] J.S. Chen, Natural frequencies and stability of an axially traveling string in contact with a stationary load system, *ASME Journal of Vibration and Acoustics* 119 (1997) 152–157.
[11] L. Zhang, J.W. Zu, Nonlinear vibrations of viscoelastic moving belts, part I: free vibration analysis, *Journal of Sound and Vibration* 216 (1998) 75–91.
[12] L. Zhang, J.W. Zu, Nonlinear vibrations of viscoelastic moving belts, part II: forced vibration analysis, *Journal of Sound and Vibration* 216 (1998) 93–105.

[13] F. Pellicano, F. Vestroni, Nonlinear dynamics and bifurcations of an axially moving beam, *ASME Journal of Vibration and Acoustics* 122 (2000) 21–30.
[14] W.T. van Horssen, On the influence of lateral vibrations of supports for an axially moving string, *Journal of Sound and Vibration* 268 (2003) 323–330.
[15] M. Pakdemirli, H. Boyaci, Effect of non-ideal boundary conditions on the vibrations of continuous systems, *Journal of Sound and Vibration* 249 (2002) 815–823.
[16] C. Shin, W. Kim, J. Chung, Free in-plane vibration of an axially moving membrane, *Journal of Sound and Vibration* 272 (2004) 137–154.
[17] W. Zhu, C.D. Mote Jr., Free and forced response of an axially moving string transporting a damped linear oscillator, *Journal of Sound and Vibration* 177 (1993) 591–610.
[18] K.Y. Lee, A.A. Renshaw, Solution of the moving mass problem using complex eigenfunction expansions, *ASME Journal of Applied Mechanics* 67 (2000) 823–827.
[19] L. Meirovitch, A new method of solution of the eigenvalue problem for gyroscopic systems, *AIAA Journal* 12 (1974) 1337–1342.
[20] G.M.T. D'Eleuterio, P.C. Huges, Dynamics of gyroelastic continua, *ASME Journal of Applied Mechanics* 51 (1984) 415–422.